TITLE:

Mcam stabilizes luminal progenitor breast cancer phenotypes via Ck2 control and Src/Akt/Stat3 attenuation

AUTHORS AND AFFILIATIONS:

Ozlen Balcioglu[1,2,*], Brooke L. Gates[1,2,*], David W. Freeman[1,2], Berhane M. Hagos[3], Elnaz Mirzaei Mehrabad[4], David Ayala-Talavera[1,2] and Benjamin T. Spike[1,2,4]

[1]Huntsman Cancer Institute, University of Utah, Salt Lake City, UT 84112 USA

[2]Department of Oncological Sciences, University of Utah, Salt Lake City, UT 84112 USA

[3]Current Address: Emergency Medicine, Oregon Health & Science University School of Medicine, Portland, OR 97239 USA

[4]School of Computing, University of Utah, Salt Lake City, UT 84112 USA

*Co-equal authorship

Corresponding Author: Benjamin T. Spike

Corresponding Author Email: Benjamin.Spike@hci.utah.edu

KEYWORDS: MCAM, Breast Cancer, Cell State, Plasticity

Running title: Mcam governs luminal breast cancer cell states via Ck2/Stat3

HIGHLIGHTS

- Mcam is expressed by diverse breast cancer subtypes.
- Mcam regulates breast cancer cell state plasticity.
- Mcam maintains the mammary luminal progenitor state.
- Mcam attenuates Stat activity.
- Mcam dictates Ck2 substrate utilization.

ABSTRACT

Breast cancers are categorized into subtypes with distinctive therapeutic vulnerabilities and prognoses based on their expression of clinically targetable receptors and gene expression patterns mimicking different cell types of the normal gland. Here, we tested the role of Mcam in breast cancer cell state control and tumorigenicity in a luminal progenitor-like murine tumor cell line (Py230) that exhibits lineage and tumor subtype plasticity. Mcam knockdown Py230 cells show augmented Stat3 and Pi3K/Akt activation associated with a lineage state switch away from a hormone-sensing/luminal progenitor state toward alveolar and basal cell related phenotypes that were refractory to growth inhibition by the anti-estrogen therapeutic, tamoxifen. Inhibition of Stat3, or the upstream activator Ck2, reversed these cell state changes. Mcam binds Ck2 and acts as a regulator of Ck2 substrate utilization across multiple mammary tumor cell lines. In Py230 cells this activity manifests as increased mesenchymal morphology, migration, and Src/Fak/Mapk/Paxillin adhesion complex signaling *in vitro*, in contrast to Mcam's reported roles in promoting mesenchymal phenotypes. *In vivo*, Mcam knockdown reduced tumor growth and take rate and inhibited cell state transition to Sox10+/neural crest like cells previously been associated with tumor aggressiveness. This contrasts with human luminal breast cancers where MCAM copy number loss is highly coupled to Cyclin D amplification, increased proliferation, and the more aggressive Luminal B subtype. Together these data indicate a critical role for Mcam and its regulation of Ck2 in control of breast cancer cell state plasticity with implications for progression, evasion of targeted therapies and combination therapy design.

1. INTRODUCTION

Breast cancers exhibit cellular and subtype heterogeneity that complicate treatment and contribute to disease progression. Whereas hormone receptor positive (HR+) and Her2 amplified (Her2+) cancers are treated with molecular therapies targeting their molecular drivers, triple negative breast cancers (TNBC) lack these molecular targets.[3] Transcriptional profiling has identified intrinsic breast cancer subtypes that partially overlap with these clinical subtype designations and with cellular compartments of the normal breast.[4] For instance, Luminal A and B subtypes are typically HR+ (estrogen and/or progesterone receptor expressing), the

56 ‘Her2-enriched’ intrinsic subtype comprises most Her2 amplified tumors, and the ‘Basal-like’ designation
57 encompasses most TNBCs.[5]

58 The origins of this heterogeneity remain controversial, and the molecular mediators are incompletely
59 understood. However, it is generally held that tumor subtype reflects particular combinations of driver
60 mutations and intrinsic characteristics of the cell of origin.[3,6,7] As such, experiments in mice targeting drivers to
61 different mammary gland cell types give rise to different subtypes of breast cancer.[8,9] Nevertheless, cell
62 plasticity has emerged as a significant contributor to intra- and inter-tumoral heterogeneity, likely playing a
63 crucial role in therapy resistance, dormancy, and metastasis in breast and other cancers.[10,11] Examples include
64 epithelial-to-mesenchymal transition (EMT)—a classic plasticity mechanism implicated in tumor cell migration,
65 invasion, and metastasis[9,12]—and cell lineage switching within the epithelial compartment, a well-documented
66 mechanism of therapy evasion and progression in diverse cancers.[13-15] Thus, hormone-dependent cancers can
67 sometimes transition into hormone-independent phenotypes that evade conventional hormone-blocking
68 therapy. In breast cancer, this conversion has been associated with EMT or alternatively a state transition to a
69 hormone insensitive, alveolar progenitor program classically driven by Elf5, and Stat3/5.[16-18] Identifying and
70 understanding the molecular regulators of epithelial lineage plasticity in breast and other cancers could reveal
71 strategies to maintain therapy sensitivity or uncover new therapeutic vulnerabilities. In this regard, we chose to
72 examine the membrane-integral, cell-surface glycoprotein MCAM (CD146; MUC18; S-Endo-1; and Gicerin) as
73 a regulator of epithelial plasticity in breast cancer based on several prior observations. Our prior studies
74 showed that Mcam is broadly expressed in multipotent fetal mammary stem cells.[1] Mcam is an established
75 marker of pericytes noted for their high intrinsic cellular plasticity, although lower-level expression in a variety
76 of other cells and tissues, including multipotent mammary stem cell and luminal progenitor (LP) compartments,
77 has been reported.[19,20] MCAM is upregulated in a variety of cancers and has different activities depending on
78 the target cancer/cell type.[19,21] In breast cancers, elevated expression of MCAM has been associated with the
79 Basal-like subtype and poor prognosis.[19,22] Experimental overexpression (OE) of MCAM in MCF7 and SKBR-3
80 cells (HR+ and HER2+ cell lines, respectively) drives EMT and enhances tumorigenesis in xenograft settings.[23]
81 However, MCAM has also been reported to be tumor suppressive and recent work has challenged the notion
82 that it is widely oncogenic.[24]

83 Mechanistically, MCAM has been implicated in a variety of biological processes relevant to mammary
84 development, cell identity, and cancer. MCAM can mediate cell-cell interactions between heterotypic cells
85 during extravasation of immune and tumor cells and promotes homotypic cell interactions through cognate
86 binding partners that are yet to be identified.[19] MCAM binds S100A8/9, Galectin-1/3 and Laminin-α4 as
87 extracellular ligands and regulates Integrin β1 and CD44 levels on the cell surface.[25-27] Inside the cell, MCAM
88 regulates integrin-mediated signaling through PIP2 and FAK activation, and ERM binding, and cooperates in
89 trafficking of a discrete internalized organellar structure associated with Wnt-mediated planar cell polarity.[28-30]
90 The MCAM cytoplasmic tail possesses putative binding/phosphorylation sites for Src family kinases, PKA, PKC
91 and CK2 that may orchestrate coupling and sequestering of broad-spectrum kinases to and from their
92 targets.[31] To date, it is unknown how these signals are integrated into cell fate choices, particularly in luminal
93 breast cancer cells where MCAM has thus far only been studied under conditions of acquired or experiment
94 OE.[19,23,29,31]
95 In the present study, using a LP/stem cell-like mammary tumor cell line derived from the MMTV-PyMT
96 mouse model (Py230) that exhibits lineage and tumor subtype plasticity and comparing this to a number of
97 additional cell lines and human archival tumor data, we found that Mcam is a potent regulator of breast cancer
98 cell state, therapy resistance and tumorigenicity.[9] Mcam's effects are mediated by its governance of the master
99 regulatory kinase Ck2. Mcam KD altered Ck2 substrate utilization, including its activation of Stat3 and
100 inactivation of PTEN. Inhibition of Ck2/Stat3 reversed these signaling and transcriptional state changes, and
101 the associated insensitivity to tamoxifen—a common characteristic of human Luminal B breast cancers which
102 we note often harbor MCAM loss. These results may inform the development of combination breast cancer
103 therapies that incorporate MCAM and/or CK2 and STAT inhibitors with existing molecularly targeted therapies
104 and point to opportunities as well as potential challenges in clinical management of breast cancer.
105

106 ## 2. METHODS

107

108 ### 2.1. Cell lines and Cell culture:

109 Met-1 and NDL-1 cell lines were provided by Dr. Alexander Borowsky.[32,33] Authenticated 4T1 (RRID:

110 CVCL_0125), E0771 (RRID: CVCL_GR23), MCF10A (RRID: CVCL_0598), MDA-MB-231 (RRID: CVCL_0062)
111 and MDA-MB-468 (RRID: CVCL_0419) cell lines were obtained from ATCC. 4T1, E0771, NDL-1, Met-1, MDA-
112 MB-231, and MDA-MB-468 cells were cultured in Dulbecco's modified Eagle's media (DMEM) with
113 ciprofloxacin 10 µg/ml and 10% fetal calf serum. MCF10A cells were cultured in Dulbecco's modified Eagle's
114 medium/F12 with 5% horse serum, 10 µg/ml insulin, 20 ng/ml epidermal growth factor, 100 ng/ml cholera toxin,
115 0.5 µg/ml hydrocortisone, and 10 µg/ml ciprofloxacin. Py230 cell line was kindly provided by L. Ellies [9]. Identity
116 of gifted lines is authenticated herein through molecular assays (e.g., scRNASeq,) that match profiles reported
117 for these lines. Passage numbers were tracked and minimized, and experiments were repeated 2-8 times
118 including repetition with early passage frozen aliquots. Py230 cells were cultured in "Py230 Media" composed
119 of F12-Kaighn's Modified Media with 5% fetal calf serum, ciprofloxacin 10µg/ml, amphotericin B 2.5µg/ml, and
120 Mito+ serum extender (Corning #355006). Py230 organoids were cultured in Py230 media with 4% Matrigel.
121 HCI-011 organoids were kindly provided by Dr. Alana Welm and cultured according to their published
122 protocol.[34] They were grown in PDxO base medium (Advanced DMEM/F12 with 5% FBS, 10 mM HEPES, 1×
123 Glutamax, 1 µg ml^{-1} hydrocortisone, 50 µg ml^{-1} gentamicin and 10 ng ml^{-1} hEGF) with 10µM Y-27632, 100 ng
124 ml^{-1} FGF2 and 1 mM NAC. All cells were grown in sterile humidified tissue culture incubators at 37 °C with 5%
125 CO_2 and ambient (~ 17–18%) O_2. Cells were transduced with lentiviral concentrates in the presence of 7 µg/ml
126 polybrene for up to 16 h with transduction efficiency (not shown) suggesting MOI <<1. CX-4945/Silmitasertib
127 (Selleck Chem #S2248), (E/Z)-GO289 (MedChem Express, #HY-115519), Ag490 (Selleck Chem #S1143),
128 Stattic/S7947 (S7947, Sigma Aldrich #19983-44-9), and tamoxifen citrate (Selleck Chem #S1972) were
129 resuspended in DMSO according to manufacturers' recommendations and diluted to final concentrations in
130 media immediately prior to being added to cells.
131
132 **2.2. Lentiviral vectors:**
133 Viral vector plasmids were obtained from OriGene Technologies, Inc. (Rockville, MD), including the mouse
134 Mcam shRNA lentiviral plasmid (Cat # TL514377), a scrambled shControl, and a custom shRNA-resistant (via
135 silent-mutation) mouse Mcam construct subcloned into a lentiviral gene expression vector (pLenti-C-mCFP-
136 P2A-BSD), (# PS100107). Completed vectors were sequenced confirmed.
137

138 **2.3. siRNA construct:**

139 siRNA constructs were obtained from OriGene Technologies, Inc. (Rockville, MD). This includes the three
140 unique 27mer mouse Mcam siRNA duplexes (SR418656A-C) and a Trilencer-27 Universal Scrambled
141 Negative Control siRNA Duplex (SR30005). Cells were transfected utilizing Lipofectamine 3000 Transfection
142 Reagent (Invitrogen, #L3000008) according to manufacturer's instructions.

143

144 **2.4. Western Blot:**

145 Cell were lysed in RIPA buffer (1X PBS (137mM NaCl; 2.7mM KCl; 4.3mM Na2PO4; 1.47 mM KH2PO4) with
146 1% Nonidet P-40 Substitute (Sigma #74385), 0.5% Sodium deoxycholate, 0.1% SDS) with the Halt Protease &
147 Phosphatase inhibitor cocktail (Thermo Fisher Scientific, #78440) , quantified with the RC-DC Protein
148 Quantification Assay (BioRad) and equivalent concentrations (10-16ug) loaded per sample on precast
149 NuPAGE 4-12% Bis-Tris gradient gels (Invitrogen). Separated proteins were transferred to nitrocellulose and
150 probed overnight with primary antibodies under agitation. Secondary antibodies were incubated with blots for
151 1hr. Intervening washes used TBST pH7.5 (10mM Tris, 15mM NaCl, 0.05%Tween 20), Blots were imaged on
152 an Odyssey CLx Imager (LI-COR).

153

154 **2.5. Immunoprecipitation:**

155 HEK293A cells were transfected with ps14-Mock [35], an rTA expression construct to later induce CK2
156 expression, utilizing Lipofectamine 3000 (Invitrogen; L3000008). 16 hours later cells were sorted for GFP+
157 cells and plated. After 32 hours cells were transfected with an equimolar mix of CK2α/β plasmid (Addgene;
158 #27093) and the relevant MCAM tail variant. Following another 16-hour incubation cells were treated with
159 DOX. After 24 hours cells were washed with PBS+EDTA, collected, resuspended in IP Lysis buffer (Pierce;
160 87787) with the Halt Protease & Phosphatase inhibitor cocktail (Thermo Fisher Scientific, #78440) and allowed
161 to rotate at 4°C for 1 hour. 10ug of rabbit anti-FLAG antibody (Invitrogen; #740001) was added and allowed to
162 incubate overnight at 4°C. The following day, magnetic Protein A/G beads (Pierce; 88802) were added
163 according to the manufacturer's instructions and samples were rotated at 4°C for 1 hour prior to magnetic
164 separation, washing the A/G beads, and sample preparation for western blot analysis. Westerns were probed
165 for HA-Tag (Invitrogen; #26183) and Myc (Invitrogen; #MA1-980) for CK2 α and β respectively.

166 **2.6. Immunohistochemistry:**

167 Freshly dissected tissues were fixed overnight at 4°C in 10% neutral buffered formalin (Sigma; HT501128).
168 Fixed tissues were transferred to 70% ethanol for storage at 4 °C. Processing for histology followed standard
169 protocols with paraffin embedding, sectioning at 5 µm thickness, baking for 1 h at 55 °C, and deparaffinizing
170 with CitriSolv (Decon Labs, 89426-268) and rehydration through graded alcohol/water washes. Antigen
171 retrieval was achieved by boiling samples 15min in citrate buffer (10 mM citric acid, 0.05% Tween 20, pH 6.0)
172 prior to overnight primary antibody staining. Slides were mounted in Fluormount-G (Electron Microscopy
173 Sciences). Slides were imaged on a Leica SP8 White light Laser Confocal microscope.

174

175 **2.7. Antibodies:**

Antibody	Clone	Manufacturer	Catalogue #	Assay	Dilution	RRID
anti-Akt	40D4	Cell Signaling Technology	2920	Western Blot	1:2000	AB_1147620
anti-phospho-Akt (Ser473)	D9E	Cell Signaling Technology	4060	Western Blot	1:2000	AB_2315049
anti-β-actin	W16197A	Biolegend	664802	Western Blot	1:2000	AB_2721349
anti-phospho-Stat3 (Tyr705)	D3A7	Cell Signaling B1:H36Technology	9145	Western Blot	1:1000	AB_2491009
anti-Stat3	124H6	Cell Signaling Technology	9139	Western Blot	1:1000	AB_331757
anti-Fyn	E3	Santa Cruz Biotechnology	SC-365913	Western Blot	1:500	AB_10842309
anti-Lyn	C13F9	Cell Signaling Technology	2796T	Western Blot	1:1000	AB_2138391
anti-phospho-src-famly (Tyr418)	EP503Y	Abcam	Ab40660	Western Blot	1:1000	AB_776106
anti-Mcam	281	Novus Biologicals	NBP2-90721	Western Blot	1:1000	unavailable
anti-MCAM	EPR3208	Abcam	Ab75769	Western Blot	1:1000	AB_2143375
anti-phospho-Pten (Ser380/Thr382/383)	44A7	Cell Signaling Technology	9549	Western Blot	1:1000	AB_659891
anti-Pten	A2B1	Santa Cruz Biotechnology	SC-7974	Western Blot	1-500	AB_628187
anti-phospho-Fak (Ty925)	polyclonal	Cell Signaling Technology	3284	Western Blot	1:1000	AB_10831810
anti-phospho-Fak (Tyr397	D20B1	Cell Signaling Technology	8556	Western Blot	1:1000	AB_10891442
anti-Fak	polyclonal	Cell Signaling Technology	3285	Western Blot	1:1000	AB_2269034
anti-phospho-Stat5 (Tyr694)	D47E7	Cell Signaling Technology	4322	Western Blot	1:400	AB_10544692
anti-Stat5	ST5-8F7	Thermo Fisher Scientific	33-5900	Western Blot	1:200	AB_2533129
anti-Rabbit-IgG-AF680	polyclonal	Thermo Fisher Scientific	A-21076	Western Blot	1:1000	AB_2535736
anti-Mouse-IgG-AF790	polyclonal	Thermo Fisher Scientific	A11375	Western Blot	1:1000	AB_2534146
anti-Rat-IgG-H&LDyLight-800	polyclonal	Thermo Fisher Scientific	SA5-10032	Western Blot	1:10000	AB_2556612
anti-Paxillin	Y113	Abcam	Ab32084	Western Blot	1:5000	AB_779033

HA-Tag	2-2.2.14	Invitrogen	26183	Western Blot	1:1000	AB_10978021
c-Myc	9E10	Invitrogen	MA1-980	Western Blot	1:1000	AB_558470
phospho-CK2 substrate	MultiMab	Cell Signaling Technology	8738S	Western Blot	1:1000	AB_2797653
anti-Sox10	SD204-04	Thermo Fisher Scientific	MA5-32398	Immunocytochemistry	1:50	AB_2809676
anti-Krt14	LL002	Thermo Fisher Scientific	MA5-11599	Immunocytochemistry	1:50	AB_10982092
anti-Krt8	TROMA-1	DSHB U of Iowa	Ab-531826	Immunocytochemistry	1:50	AB_531826
anti-Rabbit-IgG-AF568	polyclonal	Thermo Fisher Scientific	A-11011	Immunocytochemistry	1:200	AB_143157
anti-Mouse-IgG-AF647	polyclonal	Thermo Fisher Scientific	A28181	Immunocytochemistry	1:200	AB_2536165
anti-Rat-IgG-AF647	polyclonal	Thermo Fisher Scientific	A-21247	Immunocytochemistry	1:200	AB_141778
anti-Mcam	ME9F1	Biolegend	313605	FACS	1:100	AB_345299
anti-CD326	G8.8	Thermo Fisher Scientific	25-5791-80	FACS	1:160	AB_1724047
anti-Sca1	D7	Thermo Fisher Scientific	17-5981-81	FACS	1:300	AB_469486
anti-Ncam1	EPR21827	Abcam	Ab220360	FACS	1:500	AB_2927664
rabbit anti-FLAG	polyclonal	Invitrogen	740001	Immunoprecipitation	1:50	AB_2610628

2.8. scRNA Sequencing:

All protocols used to generate scRNA-seq data on 10x Genomics Chromium Controller platform including library prep, instrument and sequencing setting can be found on: https://www.10xgenomics.com/support/single-cell-gene-expression/documentation. The Chromium Next GEM Single Cell 3' Kit v3.1 (PN-1000268) was used to barcode individual cells with 16nt 10x Barcode, to tag cell specific transcript molecules with 12 nt Unique Molecular Identifier (UMI) and to capture poly (A) mRNA with 30 nt ploy(dT) sequence according to the manufactures. The following protocol based on 10x Genomics user guide (CG000315) was performed by High-Throughput Genomics Shared Resource at Huntsman Cancer Institute, University of Utah. Briefly, Py230 single cell suspension was isolated by trypsinization and resuspended in phosphate buffered saline with 0.04% bovine serum albumin. The cell suspension was filtered through 40-micron cell strainer. Viability and cell count were assessed on Countess 2 (Invitrogen, Carlsbad, CA). Equilibrium to targeted cell recovery of 6,000 cells along with 10x Gel Beads and reverse transcription reagents were loaded to Chromium Single Cell Chip G (PN-1000120) to form Gel-Bead-In Emulsions (GEMs), the nano-droplets. Within individual GEMs, barcoded cDNA generated from captured mRNA was synthesized by reverse transcription at the setting of 53°C for 45 min followed by 85°C for 5 min. Subsequent fragmentation, end repair and A-tailing, adaptor ligation and sample indexing with dual index (PN-1000215) were performed in bulk according to the user guide. The resulting

193 barcoded libraries were qualified using Agilent D1000 ScreenTape on Agilent Technology 2200 TapeStation
194 system and quantified by quantification PCR using KAPA Biosystems Library Quantification Kit for Illumine
195 Platforms (KK4842). Multiple libraries were then normalized, pooled and sequenced on NovaSeq 6000 with
196 150x150 paired end mode.
197
198 **2.9. Bulk RNA-sequencing:**
199 RNA was collected from snap frozen biological replicates of 10e6 Py230 shControl/shMcam cell-derived
200 tumors that were collected 12-weeks after inoculation. RNA was isolated via QIAzol-chloroform extraction
201 followed by column-based purification and On-Column DNase Digestion (Qiagen #79254). The aqueous phase
202 was brought to a final concentration of 50% ethanol, and RNA was purified using the RNeasy Lipid Tissue Mini
203 Kit according to the manufacturer's instructions (Qiagen #74804). Library preparation was performed using the
204 Illumina TruSeq Stranded mRNA Library Prep with UDI (Illumina; poly(A) selection). Sequencing was
205 performed using the NovaSeq 6000 (50 x 50 bp paired-end sequencing; 25 million reads per sample).
206
207 **2.10. Bioinformatic Analysis:**
208 All downstream analysis of sequencing data was completed using Loupe Browser (6.0.0) (RRID:SCR_018555),
209 Enrichr (RRID:SCR_001575), Appyters (RRID:SCR_021245), GraphPad Prism (RRID:SCR_002798) and
210 RStudio (4.1.2) (RRID:SCR_000432). For differential gene expression analysis, we utilized the default
211 clustering method of Seurat with the Louvain algorithm to iteratively group cells together [36]. Reanalysis of
212 primary mouse mammary data from Giraddi et al. used the published diffusion map coordinates and the
213 markers Krt14, Krt8 and Wfdc18, to designate 4 adult groups/cell-types, basal, luminal differentiated, luminal
214 progenitor, and alveolar [1]. We used the Seurat default differential expressed gene (DEG) test [FindMarkers()]
215 (non-parametric Wilcoxon rank sum test). The top 100 DEGs were then used for downstream comparative
216 analysis. From the Py230 dataset, DEG lists were generated by comparing the shCon luminal to shMcam
217 luminal clusters and similarly for the alveolar clusters identified through marker gene comparisons. We used
218 GSEA software (RRID:SCR_005724), and Molecular Signature Database (MSigDB; RRID:SCR_016863) to
219 compare gene sets with 100,000 permutations in GSEA Pre-ranked. GSEA data was plotted with GraphPad
220 Prism (RRID:SCR_002798). Kaplan Meier plots were generated using TCGA data visualized utilizing KMplot

221 and the auto-select cutoff values for Basal (3.45), Luminal A (3.35), Luminal B (3.29) and Her2 (2.97). [37].
222 Heatmaps and MCAM CNV analysis utilized the UCSC Xena Browser [38] (RRID:SCR_018938).
223
224 **2.11 Tumor studies:**
225 10-week-old nude female mice were from Charles River Laboratories (Wilmington, MA). 1,000 or 1,000,000
226 MMTV-PyMT Py230 cells were resuspended in complete Matrigel (Corning) and orthotopically injected into the
227 #4 mammary glands of mice. At endpoint, mice were euthanized according to AVMA guidelines and tissues
228 were harvested for processing. The maximum mammary tumor size permitted is 2cm diameter, which was not
229 exceeded in these studies.
230
231 **2.12. Statistics:**
232 Replicates and experimental repetition are indicated in figures and figure legends**.** For statistical analysis, One-
233 Way ANOVA with Tukey Kramer Multiple Comparisons, Repeated Measures One-Way ANOVA (Geisser-
234 Greenhouse correction) w/ Tukey multiple comparison tests, and Two-Way ANOVA with Sidak's multiple
235 comparisons were used. ** p<0.05, ** p<0.01, *** p<0.001, **** p<0.0001.* Gene mapping and differential gene
236 expression analysis utilized established default methods embedded in the Cell Ranger, CLoupe browser and
237 Seurat computational packages.
238
239 **3. RESULTS**
240 **3.1. Mcam maintains epithelial phenotypes in luminal mammary cancer cells.**
241 Although experimental OE of MCAM has been reported to drive EMT and basal phenotypes in breast
242 cancer cells [21,24], we found that diverse murine/human breast cancer cell lines and patient derived organoid
243 models expressed MCAM including luminal and LP-like models (**Fig. 1A-C**).[9,39] To test the requirements for
244 Mcam in Luminal breast cancer cell state control and tumorigenicity, we focused our initial attention on the
245 murine Py230 cell line, given its experimental tractability, LP-like phenotype, robust Mcam expression, and
246 reported subtype plasticity.[9,39] We knocked Mcam down by transient transfection with a panel of Mcam-
247 directed siRNAs (**Figs. S1A-C**) or by stable transduction with lentiviral vectors (LV) bearing an Mcam-directed
248 shRNA construct (**Figs. 1D-H, Fig. S1D-G**). Although transfection efficiency and KD were modest in transient

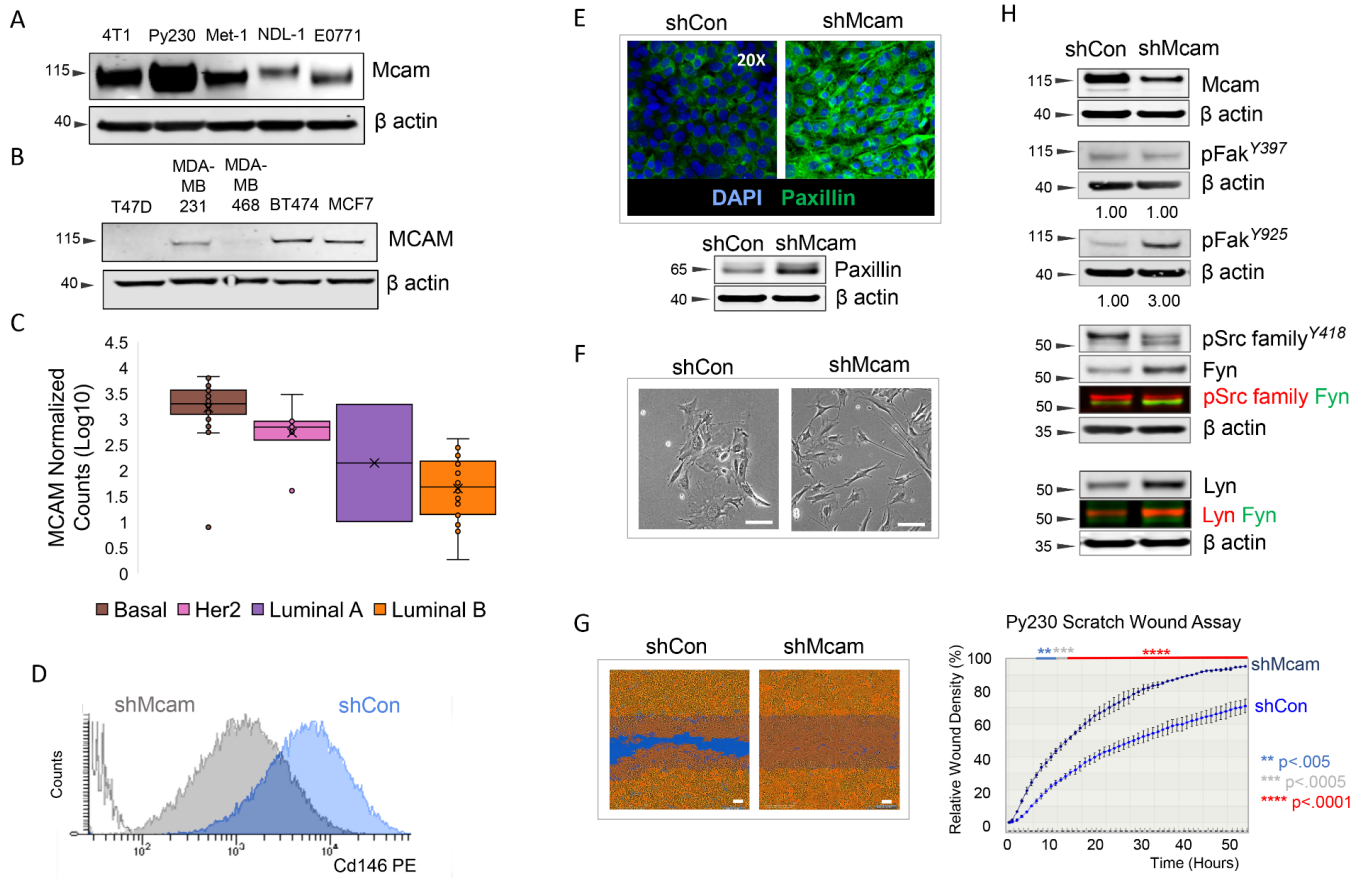

Fig. 1. Cellular and molecular signaling changes following Mcam KD in Py230 cells. A) Western blot of mouse breast cancer cell lines. B) Western blot of human breast cancer cell lines. C) Normalized MCAM counts PDM, stratified across breast cancer subtypes by PAM50 analysis. D) Surface Mcam expression (FACS) in control and Mcam KD Py230 cells. E) Representative immuno-fluorescent Paxillin staining and western blot in Mcam KD Py230 cells and scrambled controls. F) Phase contrast image of low density Mcam KD Py230 cells showing a more elongated spindeloid appearance than controls. Scale bar = 100μm. G) IncuCyte scratch wound assay indicates Mcam KD increases migration of Py230 cells. Scale bar = 100μm. Two-way ANOVA with Sidak's multiple comparisons test between shCon and shMcam. ns = not significant, *p<0.05, **p<0.01, ***p<0.001, ****p<0.0001. H) Western blot analysis of Mcam and altered focal adhesion related signaling in Mcam KD Py230 cells and scrambled controls.

transfections, a subset of cells in siMcam-transfected cultures exhibited qualitative differences in adhesion and cellular morphology with an elongated spindeloid-like phenotype (**Figs. S1A-C**). Although mesenchymal phenotypes were unexpected in KD cells, we obtained corroborating results using sorted stable LV-transduced Mcam KD Py230 cells compared to cells bearing scrambled control vectors (**Figs. 1E-H**). Three independently derived stable Mcam KD clones showed the same cellular and molecular phenotypes observed in transient KD cells including elongated cellular morphology and augmented Paxillin levels (**Figs. 1D-H, S1D-E**). Py230 shMcam cells also exhibited alterations in focal adhesion signaling including elevated activation of focal adhesion kinase and alterations in Src family kinases including Fyn and Lyn (**Fig. 1H**).[28] These changes were correlated with enhanced migration in scratch wound assays but no significant alteration to proliferation or survival relative to scrambled shRNA controls (**Fig. 1G, S1F**). However, MCAM KD did alter growth kinetics of

Py230 in 3D organoid culture as well as the 3D growth of the patient derived organoid model, HCI-011 (**Fig. S1G**).[34] These data indicate that in contrast to studies where Mcam OE drives mesenchymal phenotypes in epithelial cells, MCAM can also sustain the luminal phenotypes in breast cancer cells.

3.2. Mcam stabilizes a luminal progenitor cell state in Py230 cells.

Changes in cell morphology and morphological heterogeneity were also evident in confluent Mcam KD Py230 cultures relative to controls, suggesting alterations in cellular differentiation states or their relative distributions (**Fig. 2A**). Examination of the lineage related keratins, Krt8 and Krt14, revealed a marked

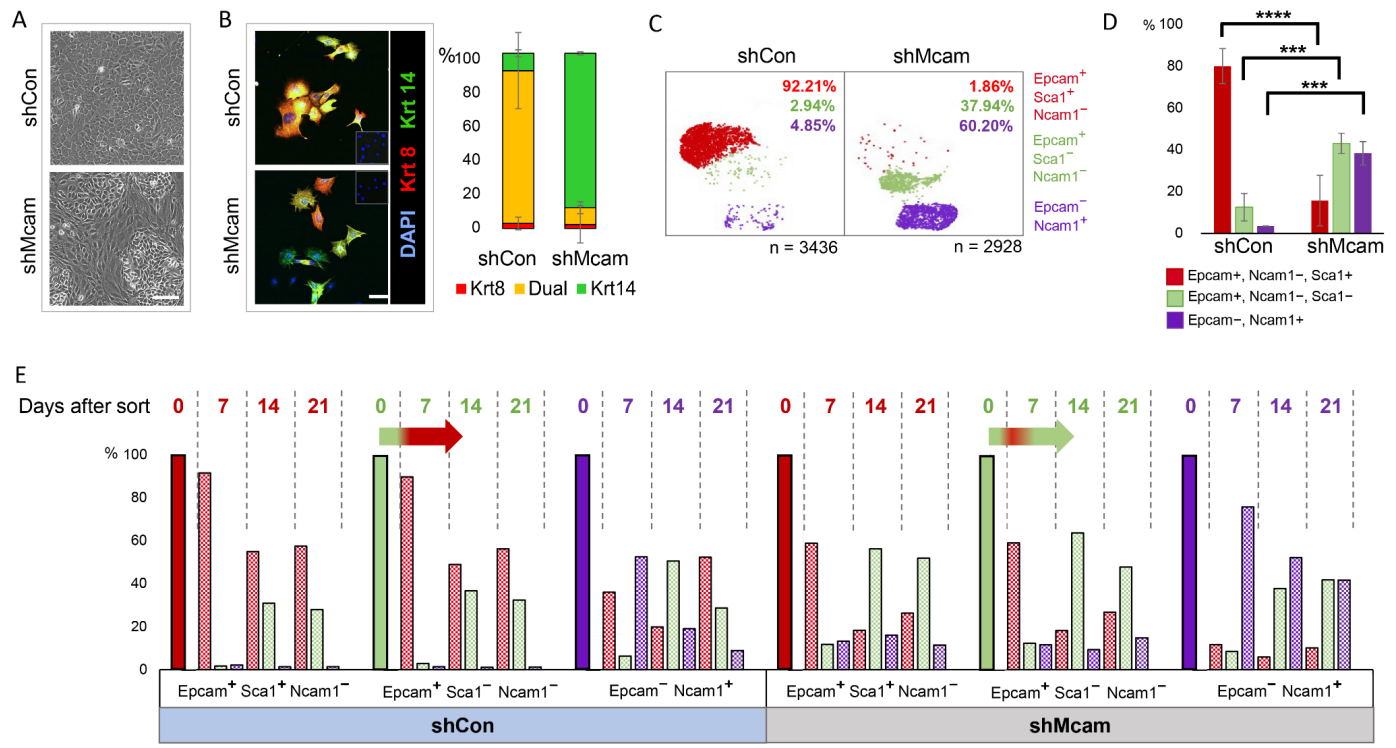

Fig. 2. Cell-state change following Mcam KD in Py230 cells. A) Phase contrast image of confluent Mcam KD and control Py230 cultures. Scale bar = 100µm. B) Altered expression of lineage associated Krt8 (red) and Krt14 (green) in Py230 Mcam KD cultures. Scale bar = 100µm. C) scRNA-seq profiles from control and Mcam KD cells reveal three major subpopulations that are identifiable by expression of previously described mammary lineage markers [2] . D) FACS analysis in triplicates confirms proportional skewing among cells expressing these three marker proteins that mirrored subpopulations identified by scRNA-seq (n=3 independent clones per genotype). Error bars = SD. Two-way ANOVA with Tukey multiple comparison test: ns = not significant, *p<0.05, **p<0.01, ***p<0.001, ****p<0.0001. E) Interconversion of Py230 subpopulations upon FACS separation and culture for 0, 7, 14 or 21 days. Horizontal arrows show immediate conversion of Epcam+Sca-Ncam- cells to Sca+ within seven days followed by reversion in to Sca- predominance in Mcam KD cells by day 14.

reduction in the frequency of uncommitted Krt8/14 co-expressing cells upon Mcam KD (**Fig. 2B**). To further characterize Mcam-associated cell state changes, we sequenced transcriptomes from several thousand individual control and Mcam KD Py230 cells (**Fig. 2C**). UMAP graphical representation of the data revealed

270 three major transcriptional cell states with differential representation between control and Mcam KD cells (**Fig.**
271 **2C, S2A,B**). Surveying the levels of previously described markers of distinct mammary cell states [2], we
272 observed that transcript levels for Epcam and Sca1 delineate the major transcriptional states identified in the
273 UMAPs as Epcam+Sca1^{High}, Epcam+Sca1^{Low} and Epcam-Sca1^{High}. We further determined that the Epcam-
274 cells are Ncam1+ whereas Epcam+ cells are Ncam- (**Fig. 2C**). Flow cytometric analysis (FACS) of surface
275 protein expression mirrored scRNA-seq data and confirmed population skewing upon Mcam KD (**Fig. 2D,**
276 **S2C,D**). FACS and scRNA-seq of additional independent clones demonstrated consistent loss of the
277 Epcam+Sca1^{High} cell state in Mcam KD cells, although some variance in the final population frequencies was
278 observed (**Figs. S2B-D**). Upon Mcam OE with a silent mutation-bearing shRNA-resistant vector in our Py230
279 Mcam KD cells, we restored predominance of the Epcam+Sca1^{High} profile while Epcam+Sca1^{low} and Epcam-
280 Ncam+ cell populations were restored to near baseline proportions (**Figs. S2E-H**). We also determined that all
281 three populations were able to interconvert and re-establish parental distributions within 3 weeks of cell sorting
282 by FACS, although kinetics for redistribution from the Epcam-Ncam+ of each genotype were slower than other
283 populations (**Fig. 2E**). Critically, while sorted Epcam+Sca1^{Low} cells of both genotypes rapidly (within one week)
284 generated Epcam+Sca1^{High} cells, the Epcam+Sca1^{High} cell type was depleted in Mcam KD cells within two
285 weeks (**Fig. 2E,** arrows). Thus, Mcam KD alters cell state distributions in Py230 by destabilizing the
286 Epcam+Sca1^{High} phenotype.
287

288 **3.3. Mcam loss triggers a Stat3 driven alveolar/basal lineage switch.**

289 Epcam and Sca1 have previously been proposed to distinguish alveolar progenitors (AP; Epcam^{high}Sca1^{low})
290 from hormone sensing luminal progenitors (HSP/LP; Epcam^{high}Sca1^{high}).[2] We took a comparative
291 transcriptomics approach to determine whether Py230 transcriptomes mimic these progenitor states more
292 broadly. We determined that Py230 cells shared expression similarity with previously published expression
293 profiles for HSP/LP transcriptional states, while the majority of Mcam KD Py230 cells resembled AP and basal
294 cell states of the normal gland (**Figs. 3A-C, S3A-C**).[1,40] Additionally, although we noted upregulation of genes
295 previously ascribed to neural crest fates in Mcam KD Py230 cells *in vivo*, we determined that several of these
296 genes are also expressed in normal mammary alveolar and basal cell types and do not necessarily indicate
297 loss of mammary epithelial specification (**Fig. 3C, S3A**).[1,40,41]

To identify underlying regulatory programs contributing to MCAM mediated cell state control, we examined

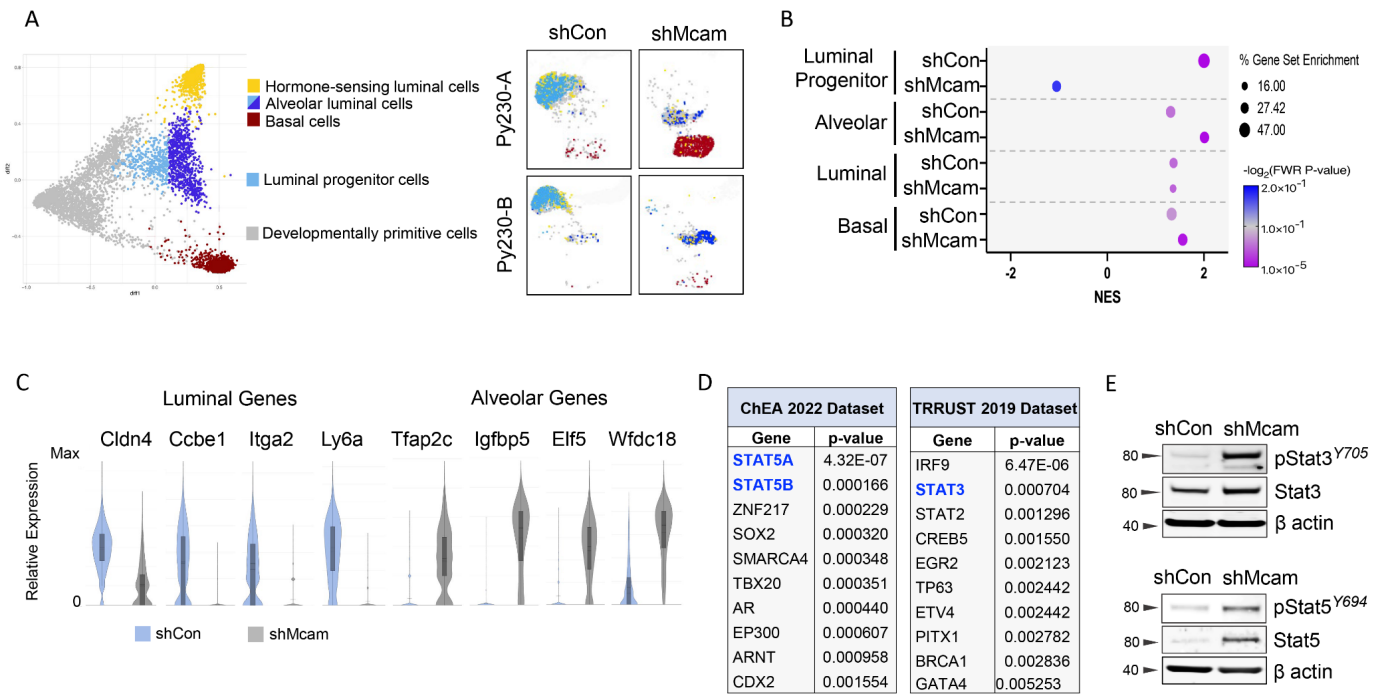

ChEA 2022 Dataset	
Gene	p-value
STAT5A	4.32E-07
STAT5B	0.000166
ZNF217	0.000229
SOX2	0.000320
SMARCA4	0.000348
TBX20	0.000351
AR	0.000440
EP300	0.000607
ARNT	0.000958
CDX2	0.001554

TRRUST 2019 Dataset	
Gene	p-value
IRF9	6.47E-06
STAT3	0.000704
STAT2	0.001296
CREB5	0.001550
EGR2	0.002123
TP63	0.002442
ETV4	0.002442
PITX1	0.002782
BRCA1	0.002836
GATA4	0.005253

Fig. 3. A luminal progenitor to alveolar/basal lineage switch accompanies MCAM loss in Py230 cells. A) The top and bottom five differentially expressed genes between the adult mammary cell types identified in the diffusion map from Giraddi et al. (left) [1],identify different cell states in Py230 control and Mcam KD cells (right). B) Gene set enrichment analysis (GSEA) showing enrichment of shCon and shMcam for luminal progenitor and alveolar cell states, respectively compared to normal mouse mammary cell populations from Giraddi et al. [1]. C) scRNA-seq analysis for relative expression of luminal and alveolar cell state markers in Py230 control (blue) and Mcam KD (grey) cells. D) Top 10 genes associated with shMcam Py230 cells from Enrichr analysis using ChEA and TRRUST datasets. E) OE and phosphorylated Stat3 and Stat5 in Py230-A cells.

enriched transcription factor target categories among genes that were differentially expressed between control and Mcam KD Py230 cells using EnrichR.[42] In addition to Elf5, a classic alveolar lineage specifier (**Fig. 3C, S3B**)[43], genes upregulated in Mcam KD cells were significantly enriched for target genes of the STAT family of transcription factors, including alveolar markers Tfap2c, Igfbp5, and Wfdc18 (**Figs. 3C,D**).[17,18,44-46] We therefore examined Stat3 and Stat5a as potential mediators of Py230 cell state change consequent to Mcam KD. Activated Stat3 and Stat5A were upregulated in Mcam KD Py230, providing a potential mechanistic basis for the alveolar cell state switch adopted by Mcam KD cells and for the OE of Stat target genes described above (**Fig. 3E, S3D-F**). While increased Stat5a could be explained by its overexpression, total Stat3 protein levels were only modestly upregulated though it was strongly overactivated in Mcam KD cells relative to MCAM expressing controls (**Fig. 3E, S3D,E**).

3.4. Mcam governs Ck2 substrate utilization attenuating Stat3 activity in Py230 cells.

To determine whether hyper-activation of Stat3 was necessary for the HSP/LP → AP switch, we treated Py230 cells with Stattic, a selective STAT3 inhibitor. Additionally, we looked at the effects of inhibitors of upstream regulators of STAT signaling including Ag490, an inhibitor of JAK2 and EGFR, and the CK2 inhibitors CX-4935 and GO289, (**Figs. 4A-E, 4G, S4A-D**).[44,47,48] Levels of phosphorylated Stat3 (pStat3) in Py230 Mcam KD cells were decreased to near baseline levels with Stattic or by inhibition of either upstream kinase (**Fig.**

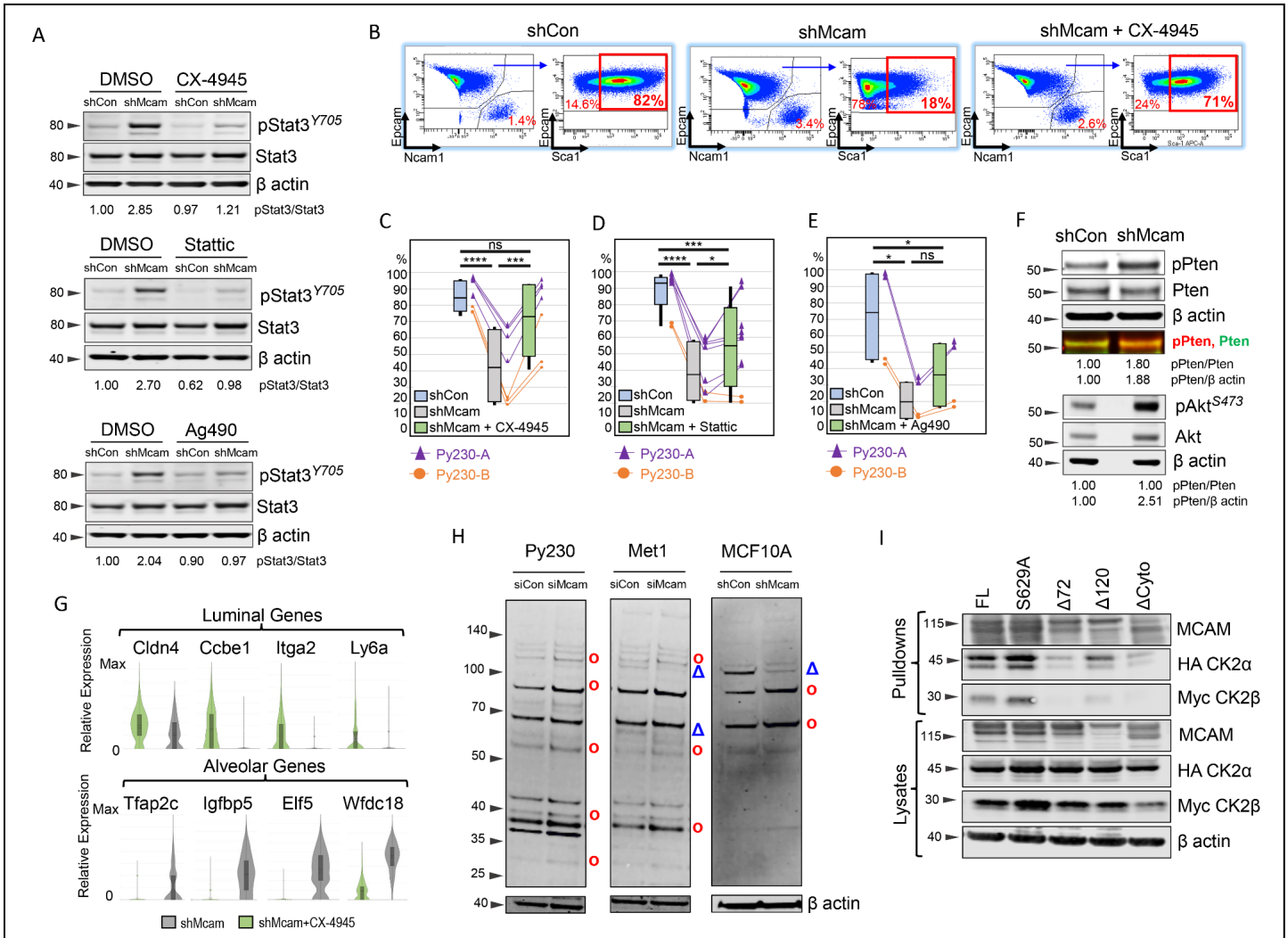

Fig. 4. Overactive CK2 in Py230 shMcam cells maintains the alveolar progenitor phenotype. A) Over-expressed and phosphorylated Stat3 in Py230-A cells and its inhibition by the kinase inhibitors, CX-4945 10μM, Ag490 50μM, Stattic 1μM for 30 minutes in WB analysis. B) Representative FACS analysis of Py230-B cells treated with CX-4945 10μM for 7 Days and stained for Epcam, Sca1 and Ncam1. C-E) Compiled FACS analysis showing the rescue of Epcam+, Sca1+ subpopulation frequencies in Py230-A and Py230-B cells treated with CX-4945 10μM for 7 Days (C), with Stattic 1μM for 7 days (D), and with Ag490 30μM for 7 days (E). RM one-way ANOVA (Geisser-Greenhouse correction) with Tukey multiple comparison test: *p<0.05, **p<0.01, ***p<0.001, ****p<0.0001. F) Western blot analysis in Py230-A cells showing higher basal levels of pPten (Ser380/Thr382/383) and pAKT in Mcam KD Py230. G) Gene expression in Py230-A cells treated with CX-4945 10μM for 7 Days (scRNA-seq). H) Western blot analysis in select breast cancer cell lines showing differential protein expression across phosphorylated CK2 substrates in siCon and siMcam transfected cell lines in culture for 48 hours post transfection or with shCon and shMCAM transduction. o=increased in MCAM KD, Δ=decreased in MCAM KD. I) Co-immunoprecipitation western blot analysis of a transiently co-transfected Flag-tagged Mcam variants and HA-Ck2a/Myc-Ck2b expression constructs in HEK293A cells. FL=full length Mcam, S629A=point mutant in the CK2 phosphorylation site of Mcam, Δ72=deletion of the distal 72 amino acids of the Mcam tail, Δ120=deletion of the membrane proximal 120 amino acids of the Mcam tail, ΔCyto=complete deletion of the cytoplasmic tail of Mcam.

316 **4A**). Cell state skewing associated with Mcam KD was dramatically reversed by CX-4945, and to a lesser
317 degree by Stattic, whereas effects of Ag490 were not significant with respect to restoration of a predominant
318 Epcam+Sca1^{High} LP-like cell state (**Figs. 4B-E, S4A,B,E-H**). Cytotoxicity was negligible for all three reagents.
319 The role of Ck2 in Mcam KD phenotypes was intriguing as CK2 has not previously been implicated as a
320 functional downstream target of MCAM, although CK2 has previously been implicated in breast tumorigenesis
321 and cell state control of mammary cells.[49,50] In previous studies, reduction of CK2 levels in the colorectal
322 cancer cell line, LoVo, led to reduced E-cadherin and other signs of EMT.[51] However, in our study, Ck2
323 inhibition did not significantly alter EMT features and Ck2 levels were unaffected by Mcam KD (**Figs. S4D,H**).
324 Rather, we noted Mcam KD was associated with augmented Ck2 activity toward Stat3 and phosphorylation of
325 the PI3K negative regulator Pten at Ck2 specific sites (Ser380/Thr382/Thr383) that promote its degradation
326 and consequent Akt hyperactivation (**Fig. 4F, S4I**).[51,52] Ck2 inhibition reversed these effects and restored
327 expression of luminal markers while depleting alveolar markers (**Fig. 4G, S4D**). These data indicate that Mcam
328 controls cell state in Py230 cells in a manner dependent on Ck2 and Stat3.
329 Using an antibody that detects phosphorylated Ck2 (pCK2) sites across diverse proteins, we observed
330 altered Ck2 phosphorylation target patterns as a function of MCAM status in a variety of lines, including Py230,
331 another PyMT derived line, Met1, and the human non-transformed epithelial cells MCF10A (**Fig. 4H, S4J,K**).
332 CX-4945 treatment confirmed Ck2 specificity of the majority of detected proteins (**Fig. S4L**). Further, Flag 'pull
333 downs' of Flag-tagged MCAM rescue constructs co-precipitated tagged CK2α/β proteins when co-expressed in
334 HEK293A cells, indicating Mcam regulation of Ck2 may be direct and dependent on the terminal 72 amino
335 acids of MCAMs' cytoplasmic (**Fig. 4I**)**.** Mutation of a putative Ck2 phosphorylation site target residue (S629A)
336 did not compromise binding (**Fig. 4I**).[31]
337
338 **3.5. MCAM loss hallmarks aggressive luminal tumors.**
339 Considering the MCAM expression we observed in luminal tumor cell lines and its activity in HSP/LP/AP cell
340 state transitions in Mcam KD Py230 cells, we re-examined MCAM's relationship to tumor aggressiveness and
341 subtype using The Cancer Genome Atlas (TCGA) database. While we confirmed that elevated MCAM levels
342 correlated with poorer prognosis in Basal-like and Her2-enriched subtypes, the inverse was true in a subset of
343 luminal cell types when examining patients treated with chemotherapy (**Fig. 5A**). Chemotherapy treated

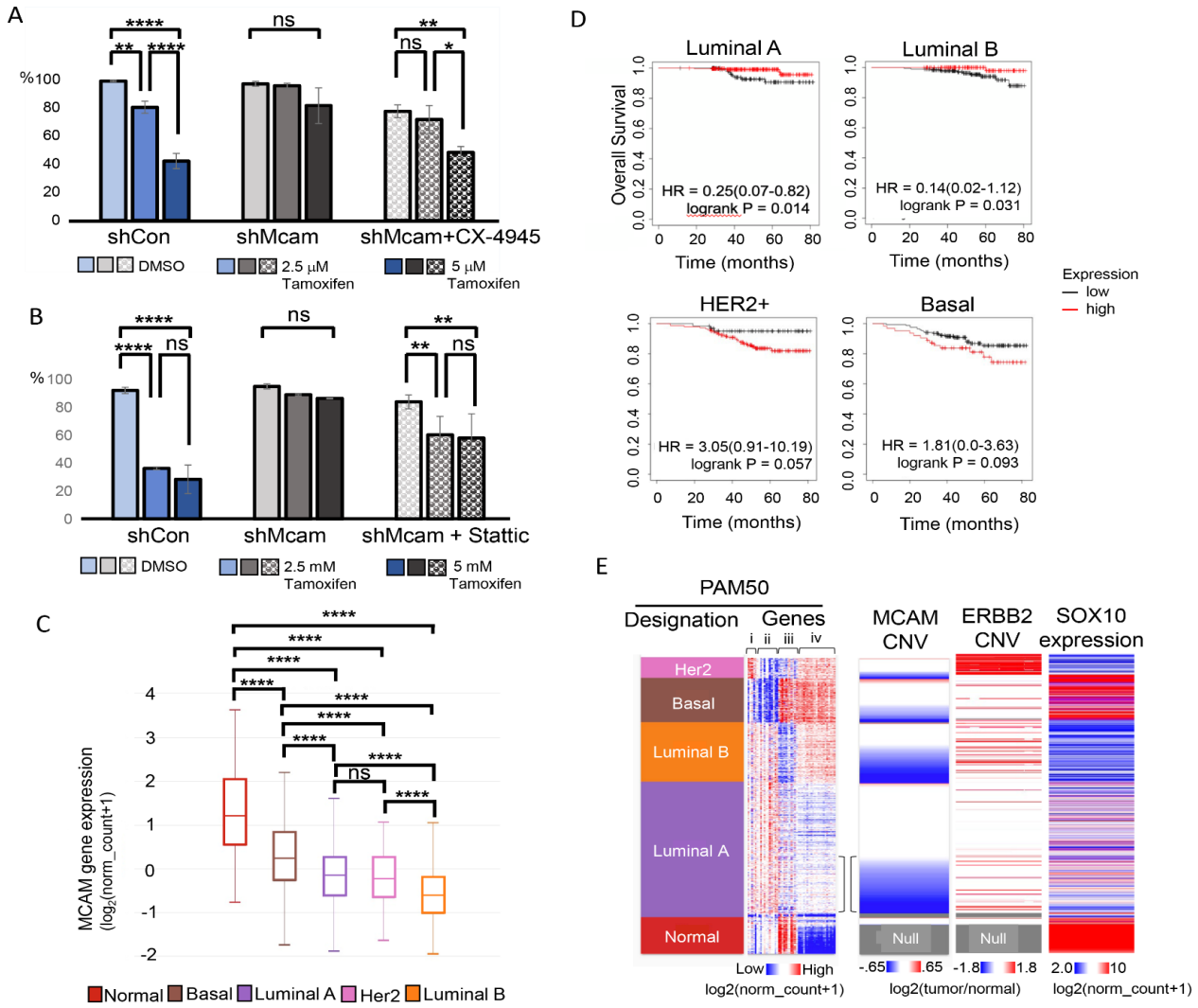

Fig. 5. MCAM loss marks aggressive luminal tumors. A-B) IncuCyte proliferation assays of Py230 control and Mcam KD cells with tamoxifen treatment shows that pretreatment with CX-4945 10μM for 7 days (A), and pretreatment with Stattic 1μM for 7 day (B) rescue the tamoxifen sensitivity in Mcam KD cells. One-Way ANOVA with Tukey Kramer Multiple Comparisons. * *p<0.05, ** p<0.01, *** p<0.001, **** p<0.0001*. C) MCAM expression across breast cancer subtypes in TCGA data. One-Way ANOVA with Tukey Kramer Multiple Comparisons. * *p<0.05, ** p<0.01, *** p<0.001, **** p<0.0001;* n=1247. D) Kaplan-Meier analysis of TCGA data breast cancer data, stratifying patients receiving chemotherapy between high and low MCAM expression. E) TCGA breast cancer data organized by PAM50 designation and MCAM copy number variation (CNV) with expression of PAM50 gene set, ERBB2 copy number variation, and SOX10 expression. The PAM 50 gene set can be broken down roughly into groups of genes related to ERBB2 expression (i), luminal genes including hormone receptor expression (ii), basal genes (iii), and proliferation genes (iv). Brackets highlight 'transitional' Luminal A with increased proliferation and MCAM CNV loss.

luminal cancers tend to reflect more aggressive tumors than those treated with endocrine therapy as an adjuvant monotherapy. Examining MCAM expression across the various breast cancer subtypes, we found that MCAM was generally reduced across all breast cancer subtypes relative to normal samples, yet more highly expressed in Basal-like, and Her2-enriched tumors than in Luminal A/B tumors as previously reported (**Fig. 5B, S5A**).[22] It should be noted that to some extent MCAM expression levels in TCGA may also reflect different levels of stromal involvement since stromal cells can express high levels of MCAM.

350 The Luminal B intrinsic subtype is distinguishable from Luminal A tumors by its poorer prognosis, more
351 frequent endocrine resistance, and greater proliferation.[3,6] However, underlying mechanisms that give rise to
352 these distinctions remain unclear. We noted that reduced MCAM gene copy number was surprisingly frequent
353 in breast cancer, especially in luminal tumors (**Fig. 5C, S5A**). In the Luminal A subtype MCAM loss was
354 associated with a trend toward increased expression of proliferation associated PAM50 genes and therefore a
355 trend toward a more Luminal B like phenotype (**Fig. 5C, S5B**).[7,38,53] This likely reflects concomitant
356 amplification of Cyclin D1 at 11q, in many cases.[53] Interestingly, among patient derived models (PDMs) that
357 formed estrogen independent outgrowths, two out of four instances showed concomitant reduction in MCAM,
358 one of which (HCI-040) showed evidence of the same 11q perturbations observed in TCGA (**Fig. S5C**).[34] We
359 also noted a correlation between MCAM copy number reduction and 'triple positive' (TPBC) status in archival
360 TCGA data (**Fig. 5C**). Clinically, despite their amplified ERBB2, such tumors are usually treated as HR+
361 luminal tumors (**Fig. 1C, S5D**).
362 Frontline treatments for luminal, HR+ breast cancers include a variety of estrogen blocking therapies such
363 as the selective estrogen receptor modulator, tamoxifen. When grown in media containing estrogens, Py230
364 cells express estrogen receptor and become estrogen sensitive.[9] In light of this, our observation that Stat3
365 inhibition reverts Mcam KD Py230 cells to an HSP/LP-related transcriptional state, and prior reports that
366 inhibition of Stat3 can increase the sensitivity to tamoxifen treatment, we tested the sensitivity of control and
367 Mcam KD Py230 cells to tamoxifen using an *in vitro* proliferation assay (**Figs. 5D,E**). We found control cells are
368 more sensitive to tamoxifen than Mcam KD cells, and that sensitivity can be restored in Mcam KD Py230 cells
369 by treatment with inhibitors of Stat3 or Ck2 (**Figs. 5D,E**). Together, these data further indicate that Mcam
370 maintains a hormone-sensing cell state through modulation of Ck2 and downstream Stat3 signaling.
371
372 **3.6. MCAM promotes tumorigenicity through cell state control.**
373 Finally, we examined whether cell state and signaling changes observed in Mcam KD cells *in vitro* alter
374 tumorigenic potential of the cells or whether they alter the neural crest associated, Basal-like, Sox10-positive
375 phenotype previously associated with Py230 cells *in vivo* (**Fig. 5C**).[39] Surprisingly, given the apparent

376 increase in mesenchymal traits observed when Mcam is KD in these cells in 2D culture, they were less
377 tumorigenic than control cells in the graft setting when low cell numbers (1,000) were injected (**Fig. 6A**). When
378 1,000,000 cells were orthotopically transplanted into the mammary fat pads, we saw formation of both control
379 and Mcam KD-derived tumors, but the tumors that form were fundamentally different in terms of size,
380 histopathological appearance, and expression of select cell type markers (**Fig. 6B**). We found that Py230 cells
381 exhibit expression of Sox10 *in vivo* though they lack such expression in 2D culture, consistent with a prior
382 report (**Fig. 6B**).[39] Sox10 expression *in vivo* marked large invasive peripheral regions of Py230 tumors
383 consistent with the previously proposed neural crest like differentiation state. We determined cells in such
384 regions co-express Krt14 suggesting they are likely basal-like or luminal progenitor-like regions (**Figs. 5C, 6B**).
385 However, these large uniform Sox10+Krt14+ positive regions were absent in Mcam KD tumors and the many
386 fewer Sox10+ cells that were found in Mcam KD tumors were usually either Krt8/14 negative or were found in
387 organized Krt8+ epithelial structures resembling the Sox10+,HR- luminal cells previously described in the
388 normal mouse mammary epithelium (**Fig. 6B**).[41] Gene expression profiling of control and Mcam KD tumors

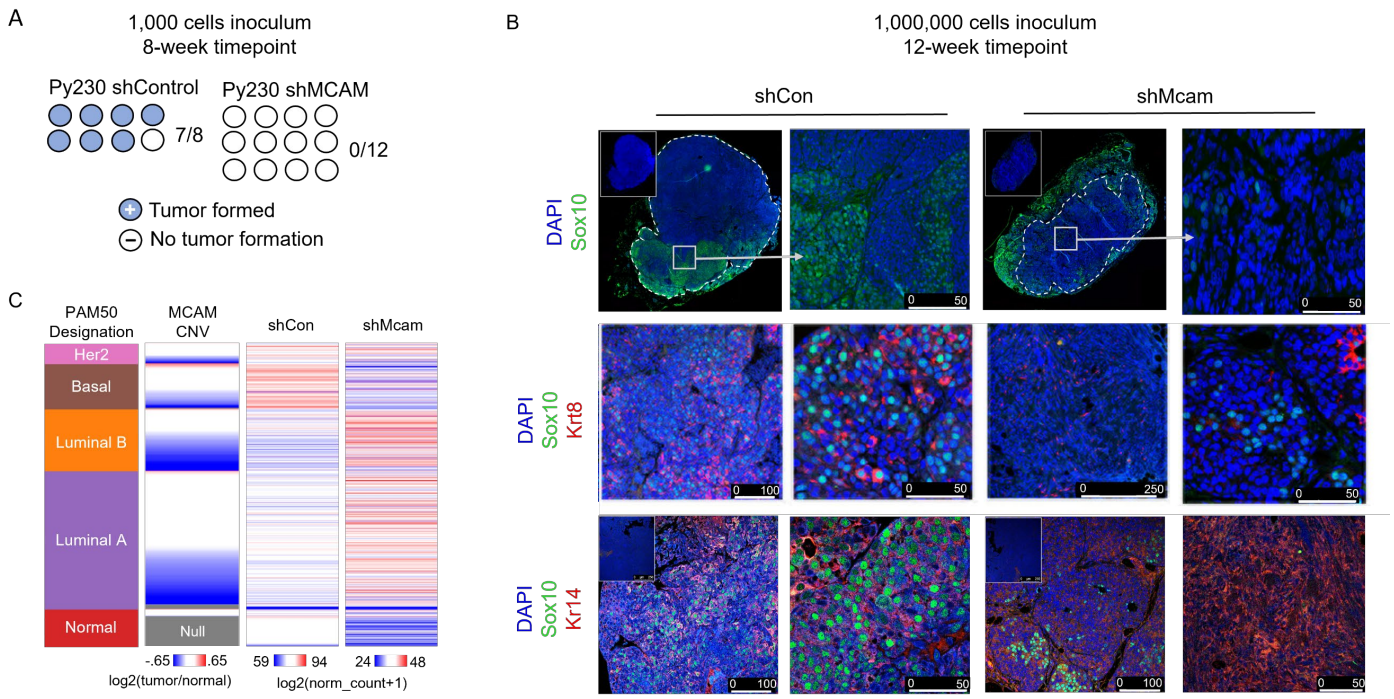

Fig. 6. Mcam promotes tumorigenic phenotypes and tumor cell plasticity. A) Reduced tumor seeding capacity of Mcam KD Py230 cells (1,000 cell orthotopic injection) after 8 weeks of growth. B) Altered cell type distribution in tumors *in vivo* generated from orthotopic injection of 10e6 Py230 control or Mcam KD cells. IHC analysis shows differential expression and distribution of cell type markers between control and Mcam KD tumors. Sox10+ stromal tumor margins are demarcated from tumor parenchyma (dashed lines). Regions of interest in low magnification images marked by white squares. C) TCGA breast cancer data organized by PAM50 designation, MCAM copy number loss, and relative expression of genes with ten greatest rank changes up or down between control and shMCAM Py230 tumor grafts (bulk RNASeq). Two-way ANOVA *p<.0001.*

389 confirmed cell state skewing by Mcam KD that was consistent with a block to the luminal progenitor related
390 basal-like phenotype (**Fig. 6C**).
391

392 **4. DISCUSSION**
393

394 Lineage plasticity is critical for proper mammary gland development and maintenance, however, in the
395 context of breast cancer, lineage plasticity could drive increased tumor heterogeneity and treatment failure [10,11].
396 Although OE of Mcam has previously been shown to promote EMT in mammary epithelial cells, here we report
397 significant Mcam expression among luminal epithelial breast cancer cell lines and the surprising finding that
398 Mcam is required to maintain the epithelial LP-like ground state of the Py230 model. This finding is consistent
399 with a recent study identifying MCAM as a marker of KRT14/KRT19 double positive LP cells of the human
400 breast [54]. Mcam KD in Py230 cells promoted differentiation toward AP/Basal phenotypes with associated
401 alterations in adhesion and motility, as well as insensitivity to tamoxifen and an apparent block to HSP-like and
402 Sox10-positive neural crest-like/basal-like breast cancer cell states.
403 Mcam effects and altered Ck2 substrate utilization while present across the different cell lines we examined,
404 appear to be cell type and breast cancer subtype specific as 1) expression in the basal-like 4T1 cell line
405 promotes, rather than inhibits, Stat3 activation, 2) several cell lines showed marginal to undetectable Stat3
406 alterations under Mcam KD, and 3) MCAM expression among HR+ breast cancer PDMs was enriched among
407 those that (like Py230) co-express ERBB2 and classify as Luminal B (**Fig. S5D** and [55]). We propose that the
408 cell type specificity of MCAM effects may reflect coupling or decoupling of CK2 (or other upstream kinases) to
409 different client proteins depending on a cell's ground state. This may be critical to understanding CK2 activity
410 and regulation as CK2 is a constitutively active high-level regulatory kinase with hundreds of substrates whose
411 mechanism of regulation and roles in mammary lineage control are not well understood, though scaffolding (for
412 instance by MCAM) represents a plausible mechanism.
413 Despite the increased mesenchymal features and therapy resistance observed for Mcam KD Py230 cells *in*
414 *vitro*, Mcam KD reduced tumorigenic seeding and growth of grafted cells in mice, a result that is at least
415 superficially consistent with prior studies correlating higher MCAM expression to tumor aggressiveness.[19,22,24]
416 However, this too may be subtype dependent as re-analysis of archival TCGA breast cancer data showed

417 MCAM expression to be a favorable marker in Luminal A and B tumors and showed MCAM loss to typify the
418 more aggressive and more frequently tamoxifen resistant Luminal B subtype as well as the more proliferative
419 (by gene signature) samples among Luminal A tumors.[38] By contrast, tumors robustly expressing MCAM are
420 typically Basal-like. It is noteworthy that recent studies suggest that the Basal-like subtype arises from LPs and
421 'involution mimicry', thus invoking a critical role for LP and AVP fate switches [43,56]. Based on our data and
422 analysis of TCGA, we speculate that MCAM may be essential for the emergence of Basal-like tumors arising
423 from the LP.
424 It should be noted that comparative transcriptomics did not indicate a strong association between Luminal B
425 tumors in TCGA and Mcam KD Py230.
426 The recurrent genetic aberration at 11q that typifies most of the TCGA breast cancers with Mcam copy number
427 reduction usually involves concomitant loss of several additional 11q genes that may contribute to cell
428 phenotype (e.g., PGR, ATM, etc.) and amplification of Cyclin D1 (**Figs. S5C,D**).[4,6,53] Thus, it is reasonable to
429 assume that several additional genetic alterations may cooperate with MCAM loss in the context of Luminal B
430 tumors in humans. Nevertheless, altered tamoxifen responses have been associated with 11q deletions in
431 human breast cancer although the specific gene(s) responsible for this effect remain uncertain.[53]
432 The findings above may be key to designing combination therapies that effectively manage shifting
433 therapeutic vulnerabilities deriving from the plastic cell state change potential of mammary luminal progenitors.
434 For instance, newer CK2 or STAT3 inhibitors may be of interest in combination with hormone receptor targeted
435 therapies for some cancers.[49,57] STATs and associated factors are not only strongly implicated in alveolar cell
436 state control in the normal gland but also have well documented roles in breast and other cancers.[18,55,57]
437 Indeed, a recent study demonstrated STAT3 inhibition can increase the tamoxifen sensitivity of tamoxifen-
438 resistant breast cancer cells.[57] Alternatively, if MCAM expression permits access to invasive neural crest like
439 states *in vivo,* it may be more effective to inhibit MCAM and seek out new vulnerabilities of the resultant
440 hormone-insensitive cell state. Altogether, our studies indicate that Mcam plays a critical role in breast cancer
441 cell state determination via Ck2 and Stat3 control, with implications for understanding developmental plasticity
442 and MCAM's role in breast cancer intra- and inter-tumoral heterogeneity.
443
444

445 **5. DECLARATIONS**

446 **Ethics approval and consent to participate:**

447 All animal care and procedures were approved and monitored by an Institutional Animal Care and Use
448 Committee.

449 **Consent for publication:**

450 Not applicable.

451 **Data Availability:**

452 Datasets generated during and/or analyzed during the current study are either publicly available (TCGA;
453 https://www.cancer.gov/tcga), are deposited at Gene Expression Omnibus (GEO) under GSE233093 or are
454 within the article and its supplementary data files. All codes and R-packages used in the study are publicly
455 available and have been disclosed in Methods or are available from the corresponding authors on reasonable
456 request.

457 **Competing interests:**

458 The authors declare no conflict of interest exists.

459 **Funding:**

460 This work was supported by the Huntsman Cancer Foundation and Halt Cancer at X Foundation.

461 **Authors' Contributions:**

462 Concept: BTS. Experimental Design: OB, BLG, BTS. Execution: OB, BLG, DWF, BH, BTS. Analysis: BLG,
463 EMM, DA-T. Interpretation: All authors. Writing: OB, BLG, BTS.

464 **Acknowledgements:**

465 We thank C. Trejo for technical assistance and M. Kruithof-de Julio, T. Oliver, and D. Salomon for valuable
466 discussions. We also acknowledge generous support from the Huntsman Cancer Foundation, and from the
467 Halt Cancer at X foundation. We thank the University of Utah/HCI Cancer Center Support Grant (P30
468 CA42014), and staff in the Flow Cytometry, HSC Cell Imaging, Preclinical Research Resource, Biostatistics,
469 High-Throughput Genomics and Bioinformatics shared core resources. Research reported in this publication
470 utilized the Preclinical Research Resource, Flow Cytometry Core, Biorepository and Molecular Pathology, and
471 High-Throughput Genomics and Bioinformatics shared resources at Huntsman Cancer Institute at the
472 University of Utah and was supported by the National Cancer Institute of the National Institutes of Health under

Award Number P30CA042014. The content is solely the responsibility of the authors and does not necessarily represent the official views of the NIH.

6. LIST OF ABBREVIATIONS:

TCGA: *The Cancer Genome Atlas*

scRNA-seq: *Single cell RNA-seq*

RNA-seq: *RNA sequencing*

KD: *Knock down*

OE: *Over expression*

shRNA: *Short hairpin RNA*

siRNA: *Small Interfering RNA*

IHC: *Immunohistochemistry*

pCK2: *Phosphorylated casein kinase 2*

GSEA: *Gene Set Enrichment Analysis*

EMT: *Epithelial-to-Mesenchymal Transition*

LP*: Luminal progenitor*

HSP: *Hormone-sensing progenitor*

AP: *Alveolar progenitor*

TPBC: *Triple Positive Breast Cancer*

TNBC: *Triple Negative Breast Cancer*

CNV: *Copy Number Variation*

ns: *not significant*

HR: *Hormone Receptor*

FDR: *False discovery rate*

NES: *Normalized enrichment score*

FACS: *Fluorescence-activated cell sorting*

ERM: *ezrin-radixin-moesin*

MMTV-PyMT: *Mouse mammary tumor virus polyomavirus middle T*

PDM: *Patient Derived Model*

7. REFERENCES

1 Giraddi, R. R. *et al.* Single-Cell Transcriptomes Distinguish Stem Cell State Changes and Lineage Specification Programs in Early Mammary Gland Development. *Cell Rep* **24**, 1653-1666 e1657 (2018). https://doi.org:10.1016/j.celrep.2018.07.025

2 Shehata, M. *et al.* Phenotypic and functional characterisation of the luminal cell hierarchy of the mammary gland. *Breast Cancer Res* **14**, R134 (2012). https://doi.org:10.1186/bcr3334

3 Testa, U., Castelli, G. & Pelosi, E. Breast Cancer: A Molecularly Heterogenous Disease Needing Subtype-Specific Treatments. *Med Sci (Basel)* **8** (2020). https://doi.org:10.3390/medsci8010018

4 Sorlie, T. *et al.* Gene expression patterns of breast carcinomas distinguish tumor subclasses with clinical implications. *Proc Natl Acad Sci U S A* **98**, 10869-10874 (2001). https://doi.org:10.1073/pnas.191367098

5 Cho, N. Molecular subtypes and imaging phenotypes of breast cancer. *Ultrasonography* **35**, 281-288 (2016). https://doi.org:10.14366/usg.16030

6 Ades, F. *et al.* Luminal B breast cancer: molecular characterization, clinical management, and future perspectives. *J Clin Oncol* **32**, 2794-2803 (2014). https://doi.org:10.1200/JCO.2013.54.1870

7 Kensler, K. H. *et al.* PAM50 Molecular Intrinsic Subtypes in the Nurses' Health Study Cohorts. *Cancer Epidemiol Biomarkers Prev* **28**, 798-806 (2019). https://doi.org:10.1158/1055-9965.EPI-18-0863

8 Smith, B. A. *et al.* Targeting the PyMT Oncogene to Diverse Mammary Cell Populations Enhances Tumor Heterogeneity and Generates Rare Breast Cancer Subtypes. *Genes Cancer* **3**, 550-563 (2012). https://doi.org:10.1177/1947601913475359

9 Bao, L., Cardiff, R. D., Steinbach, P., Messer, K. S. & Ellies, L. G. Multipotent luminal mammary cancer stem cells model tumor heterogeneity. *Breast Cancer Res* **17**, 137 (2015). https://doi.org:10.1186/s13058-015-0615-y

10 Wahl, G. M. & Spike, B. T. Cell state plasticity, stem cells, EMT, and the generation of intra-tumoral heterogeneity. *NPJ Breast Cancer* **3**, 14 (2017). https://doi.org:10.1038/s41523-017-0012-z

11 Kong, D., Hughes, C. J. & Ford, H. L. Cellular Plasticity in Breast Cancer Progression and Therapy. *Front Mol Biosci* **7**, 72 (2020). https://doi.org:10.3389/fmolb.2020.00072

12 Zhang, Y. & Weinberg, R. A. Epithelial-to-mesenchymal transition in cancer: complexity and opportunities. *Front Med* **12**, 361-373 (2018). https://doi.org:10.1007/s11684-018-0656-6

13 Zewdu, R. *et al.* An NKX2-1/ERK/WNT feedback loop modulates gastric identity and response to targeted therapy in lung adenocarcinoma. *Elife* **10** (2021). https://doi.org:10.7554/eLife.66788

14 Orstad, G. *et al.* FoxA1 and FoxA2 control growth and cellular identity in NKX2-1-positive lung adenocarcinoma. *Dev Cell* **57**, 1866-1882 e1810 (2022). https://doi.org:10.1016/j.devcel.2022.06.017

15 Wang, X. *et al.* A luminal epithelial stem cell that is a cell of origin for prostate cancer. *Nature* **461**, 495-500 (2009). https://doi.org:10.1038/nature08361

16 Chakrabarti, R. *et al.* Elf5 regulates mammary gland stem/progenitor cell fate by influencing notch signaling. *Stem Cells* **30**, 1496-1508 (2012). https://doi.org:10.1002/stem.1112

17 Haricharan, S. & Li, Y. STAT signaling in mammary gland differentiation, cell survival and tumorigenesis. *Mol Cell Endocrinol* **382**, 560-569 (2014). https://doi.org:10.1016/j.mce.2013.03.014

18 Caffarel, M. M. *et al.* Constitutive activation of JAK2 in mammary epithelium elevates Stat5 signalling, promotes alveologenesis and resistance to cell death, and contributes to tumourigenesis. *Cell Death Differ* **19**, 511-522 (2012). https://doi.org:10.1038/cdd.2011.122

19 Wang, Z. *et al.* CD146, from a melanoma cell adhesion molecule to a signaling receptor. *Signal Transduct Target Ther* **5**, 148 (2020). https://doi.org:10.1038/s41392-020-00259-8

20 Spike, B. T. *et al.* A mammary stem cell population identified and characterized in late embryogenesis reveals similarities to human breast cancer. *Cell Stem Cell* **10**, 183-197 (2012). https://doi.org:10.1016/j.stem.2011.12.018

21 Imbert, A. M. *et al.* CD146 expression in human breast cancer cell lines induces phenotypic and functional changes observed in Epithelial to Mesenchymal Transition. *PLoS One* **7**, e43752 (2012). https://doi.org:10.1371/journal.pone.0043752

22 Liang, Y. K. *et al.* MCAM/CD146 promotes tamoxifen resistance in breast cancer cells through induction of epithelial-mesenchymal transition, decreased ERalpha expression and AKT activation. *Cancer Lett* **386**, 65-76 (2017). https://doi.org:10.1016/j.canlet.2016.11.004

23 Huang, C. Y. & Wu, G. J. METCAM/MUC18 promoted tumorigenesis of human breast cancer SK-BR-3 cells in a dosage-specific manner. *Taiwan J Obstet Gynecol* **55**, 202-212 (2016). https://doi.org:10.1016/j.tjog.2016.02.010

24 Zabouo, G. *et al.* CD146 expression is associated with a poor prognosis in human breast tumors and with enhanced motility in breast cancer cell lines. *Breast Cancer Res* **11**, R1 (2009). https://doi.org:10.1186/bcr2215

25 Ruma, I. M. *et al.* MCAM, as a novel receptor for S100A8/A9, mediates progression of malignant melanoma through prominent activation of NF-kappaB and ROS formation upon ligand binding. *Clin Exp Metastasis* **33**, 609-627 (2016). https://doi.org:10.1007/s10585-016-9801-2

26 Ishikawa, T. *et al.* Laminins 411 and 421 differentially promote tumor cell migration via alpha6beta1 integrin and MCAM (CD146). *Matrix Biol* **38**, 69-83 (2014). https://doi.org:10.1016/j.matbio.2014.06.002

27 Ouhtit, A., Abdraboh, M. E., Hollenbach, A. D., Zayed, H. & Raj, M. H. G. CD146, a novel target of CD44-signaling, suppresses breast tumor cell invasion. *Cell Commun Signal* **15**, 45 (2017). https://doi.org:10.1186/s12964-017-0200-3

28 Webb, D. J. *et al.* FAK-Src signalling through paxillin, ERK and MLCK regulates adhesion disassembly. *Nat Cell Biol* **6**, 154-161 (2004). https://doi.org:10.1038/ncb1094

29 Ye, Z. *et al.* Wnt5a uses CD146 as a receptor to regulate cell motility and convergent extension. *Nat Commun* **4**, 2803 (2013). https://doi.org:10.1038/ncomms3803

30 Zhang, Q., Zhang, S., Chen, J. & Xie, Z. The Interplay between Integrins and Immune Cells as a Regulator in Cancer Immunology. *Int J Mol Sci* **24** (2023). https://doi.org:10.3390/ijms24076170

31 Wu, G.-J. METCAM/MUC18 expression and cancer metastasis. *Current Genomics* **6**, 333-349 (2005).

32 Borowsky, A. D. *et al.* Syngeneic mouse mammary carcinoma cell lines: two closely related cell lines with divergent metastatic behavior. *Clin Exp Metastasis* **22**, 47-59 (2005). https://doi.org:10.1007/s10585-005-2908-5

33 Siegel, P. M., Ryan, E. D., Cardiff, R. D. & Muller, W. J. Elevated expression of activated forms of Neu/ErbB-2 and ErbB-3 are involved in the induction of mammary tumors in transgenic mice: implications for human breast cancer. *EMBO J* **18**, 2149-2164 (1999). https://doi.org:10.1093/emboj/18.8.2149

34 Guillen, K. P. *et al.* A human breast cancer-derived xenograft and organoid platform for drug discovery and precision oncology. *Nat Cancer* **3**, 232-250 (2022). https://doi.org:10.1038/s43018-022-00337-6

35 Balcioglu, O. *et al.* CRIPTO antagonist ALK4(L75A)-Fc inhibits breast cancer cell plasticity and adaptation to stress. *Breast Cancer Res* **22**, 125 (2020). https://doi.org:10.1186/s13058-020-01361-z

36 Hao, Y. *et al.* Integrated analysis of multimodal single-cell data. *Cell* **184**, 3573-3587 e3529 (2021). https://doi.org:10.1016/j.cell.2021.04.048

37 Lanczky, A. & Gyorffy, B. Web-Based Survival Analysis Tool Tailored for Medical Research (KMplot): Development and Implementation. *J Med Internet Res* **23**, e27633 (2021). https://doi.org:10.2196/27633

38 Goldman, M. J. *et al.* Visualizing and interpreting cancer genomics data via the Xena platform. *Nat Biotechnol* **38**, 675-678 (2020). https://doi.org:10.1038/s41587-020-0546-8

39 Dravis, C. *et al.* Epigenetic and Transcriptomic Profiling of Mammary Gland Development and Tumor Models Disclose Regulators of Cell State Plasticity. *Cancer Cell* **34**, 466-482 e466 (2018). https://doi.org:10.1016/j.ccell.2018.08.001

40 Bach, K. *et al.* Differentiation dynamics of mammary epithelial cells revealed by single-cell RNA sequencing. *Nat Commun* **8**, 2128 (2017). https://doi.org:10.1038/s41467-017-02001-5

41 Dravis, C. *et al.* Sox10 Regulates Stem/Progenitor and Mesenchymal Cell States in Mammary Epithelial Cells. *Cell Rep* **12**, 2035-2048 (2015). https://doi.org:10.1016/j.celrep.2015.08.040

42 Xie, Z. *et al.* Gene Set Knowledge Discovery with Enrichr. *Curr Protoc* **1**, e90 (2021). https://doi.org:10.1002/cpz1.90

43 Valdes-Mora, F. *et al.* Single-cell transcriptomics reveals involution mimicry during the specification of the basal breast cancer subtype. *Cell Rep* **35**, 108945 (2021). https://doi.org:10.1016/j.celrep.2021.108945

44 De Vos, J., Jourdan, M., Tarte, K., Jasmin, C. & Klein, B. JAK2 tyrosine kinase inhibitor tyrphostin AG490 downregulates the mitogen-activated protein kinase (MAPK) and signal transducer and activator of transcription (STAT) pathways and induces apoptosis in myeloma cells. *Br J Haematol* **109**, 823-828 (2000). https://doi.org:10.1046/j.1365-2141.2000.02127.x

45 Yeo, S. K. *et al.* Single-cell RNA-sequencing reveals distinct patterns of cell state heterogeneity in mouse models of breast cancer. *Elife* **9** (2020). https://doi.org:10.7554/eLife.58810
46 Tai, C. I., Schulze, E. N. & Ying, Q. L. Stat3 signaling regulates embryonic stem cell fate in a dose-dependent manner. *Biol Open* **3**, 958-965 (2014). https://doi.org:10.1242/bio.20149514
47 Schust, J., Sperl, B., Hollis, A., Mayer, T. U. & Berg, T. Stattic: a small-molecule inhibitor of STAT3 activation and dimerization. *Chem Biol* **13**, 1235-1242 (2006). https://doi.org:10.1016/j.chembiol.2006.09.018
48 Zheng, Y. *et al.* A CK2-dependent mechanism for activation of the JAK-STAT signaling pathway. *Blood* **118**, 156-166 (2011). https://doi.org:10.1182/blood-2010-01-266320
49 Filhol, O., Deshiere, A. & Cochet, C. in *Protein Kinase CK2* 363-382 (2013).
50 Gray, G. K., McFarland, B. C., Rowse, A. L., Gibson, S. A. & Benveniste, E. N. Therapeutic CK2 inhibition attenuates diverse prosurvival signaling cascades and decreases cell viability in human breast cancer cells. *Oncotarget* **5**, 6484-6496 (2014). https://doi.org:10.18632/oncotarget.2248
51 Zou, J. *et al.* Protein kinase CK2alpha is overexpressed in colorectal cancer and modulates cell proliferation and invasion via regulating EMT-related genes. *J Transl Med* **9**, 97 (2011). https://doi.org:10.1186/1479-5876-9-97
52 Miller, S. J., Lou, D. Y., Seldin, D. C., Lane, W. S. & Neel, B. G. Direct identification of PTEN phosphorylation sites. *FEBS Lett* **528**, 145-153 (2002). https://doi.org:10.1016/s0014-5793(02)03274-x
53 Lundgren, K., Holm, K., Nordenskjold, B., Borg, A. & Landberg, G. Gene products of chromosome 11q and their association with CCND1 gene amplification and tamoxifen resistance in premenopausal breast cancer. *Breast Cancer Res* **10**, R81 (2008). https://doi.org:10.1186/bcr2150
54 Isberg, O. G. *et al.* A CD146 FACS Protocol Enriches for Luminal Keratin 14/19 Double Positive Human Breast Progenitors. *Sci Rep* **9**, 14843 (2019). https://doi.org:10.1038/s41598-019-50903-9
55 Hughes, K. & Watson, C. J. The Multifaceted Role of STAT3 in Mammary Gland Involution and Breast Cancer. *Int J Mol Sci* **19** (2018). https://doi.org:10.3390/ijms19061695
56 Kohler, K. T. *et al.* Ductal keratin 15(+) luminal progenitors in normal breast exhibit a basal-like breast cancer transcriptomic signature. *NPJ Breast Cancer* **8**, 81 (2022). https://doi.org:10.1038/s41523-022-00444-8
57 Moon, S. Y. *et al.* Inhibition of STAT3 enhances sensitivity to tamoxifen in tamoxifen-resistant breast cancer cells. *BMC Cancer* **21**, 931 (2021). https://doi.org:10.1186/s12885-021-08641-7